PAPER • OPEN ACCESS

In situ monitoring of artificial aging and solution heat treatment of a commercial Al–Mg–Si alloy with a high intensity positron beam

IOP ebooks™

Bringing together innovative digital publishing with leading authors from the global scientific community.

Start exploring the collection–download the first chapter of every title for free.

In situ monitoring of artificial aging and solution heat treatment of a commercial Al–Mg–Si alloy with a high intensity positron beam

L Resch[1] , T Gigl[2], G Klinser[1], C Hugenschmidt[2], W Sprengel[1] and R Würschum[1]

[1] Institute of Materials Physics, Graz University of Technology, Petersgasse 16, 8010 Graz, Austria
[2] Physics Department E 21 and FRM II, Technical University Munich, D-85747 Garching, Germany

E-mail: l.resch@tugraz.at

CrossMark

Abstract

Microstructural changes of a commercial Al–Mg–Si alloy were studied during artificial aging by *in situ* Doppler broadening spectroscopy using a high-intensity positron beam. The *in situ* positron annihilation characteristics at high temperatures differ considerably from the conventionally applied *ex situ* measurements at low temperatures. Therefore, a more comprehensive view of precipitation processes in Al–Mg–Si alloys is obtained. Further, *in situ* positron–electron annihilation techniques allow for an investigation of aging processes with increased sensitivity. For the artificial aging temperatures of 180 °C and 210 °C pronounced variations of the Doppler broadening S-parameter reveal (i) the evolution of clusters into larger precipitates and (ii) the time of the formation of β" precipitates and the role of vacancies in connection to this. Towards higher aging times, the transformation from coherent β" to semi-coherent β' precipitates could be verified. Additional insights are gained by *in situ* measurements of the S-parameter during the solution heat treatment of the previously overaged sample. Here, the S-parameter reveals both the dissolution of precipitates starting from temperatures of 364 °C and the thermal generation of vacancies.

Keywords: positron–electron annihilation, Al alloys, positron beam

(Some figures may appear in colour only in the online journal)

1. Introduction

Age-hardenable aluminium alloys have the advantage of low weight and good resistance to corrosion and hence are being used in an increasingly wide range of industrial applications [1, 2]. These alloys achieve their maximum hardness after heat treatment at elevated temperatures due to the growth of precipitates within the Al matrix, which harden the material by hindering dislocation movement. This process is referred to as artificial aging. Although Al–Mg–Si alloys were developed in the 1920s and appropriate heat treatment methods have been known for a long time [3, 4], the detailed processes controlling the change in hardness during artificial aging are still not fully understood. When the technique of age hardening is applied, the first step is to quench the alloy from the high temperature single-phase region to room temperature producing a supersaturated solid solution (SSSS). In a second step at elevated temperatures, the system transitions from the SSSS state through a series of intermediates with meta-stable precipitates, of different crystal structure and chemical

composition, towards its equilibrium phase. An approximate, generally agreed model is the following precipitation sequence [5]:

$$SSSS \rightarrow Si\text{-}, \ Mg\text{- clusters} \rightarrow \beta'' \rightarrow \beta'/U_1/U_2/B' \rightarrow \beta.$$
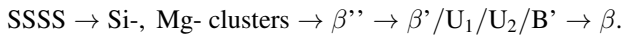
From the supersaturated solid solution Si- and Mg-clusters and co-clusters are formed during the first minutes of aging. They evolve into metastable β'' precipitates, which are coherent to the Al matrix. Due to their coherence β'' precipitates make a major contribution to the hardness of the alloy. They are found to be the dominant type of precipitate in samples exhibiting maximum hardness [6]. The crystal structure of β'' precipitates was determined to be monoclinic using transmission electron microscopy (TEM) and quantitative electron diffraction refinements [7]. Their composition most likely, is $Mg_4Al_3Si_4$ as revealed by scanning transmission electron microscopy [8]. After longer aging times the β'' precipitates transform into β', U_1, U_2 and B' precipitates, which can coexist in the alloy and are semi-coherent to the Al matrix [9]. The β' phase is predominant among those phases and therefore best known. It has been determined by electron diffraction measurements and first principles calculations that β' precipitates are of hexagonal crystal structure and do not contain Al (composition of β': Mg_9Si_5) [10]). On the other hand, the U_1, U_2 and B' precipitates contain varying amounts of Al and differ in their crystal structures [6, 11, 12]. Whether and to what extent U_1, U_2 and B' precipitates are formed during aging is strongly dependent on the exact composition of the alloy and the previous heat treatment. The final stage in the precipitation sequence is the equilibrium phase β (Mg_2Si). The β precipitates appear after several days of artificial aging. They are incoherent to the Al matrix and have a face centered cubic crystal structure [13].

Apart from the above mentioned methods, the sequence and compositions of precipitates following the β'' phase can be observed experimentally by various other techniques such as differential scanning calorimetry (DSC) [14] or atom probe tomography [11]. Initial clustering of few atoms, which proceeds on very short timescales, as well as transitions between different precipitation stages are difficult to resolve by established techniques. However, due to their strong influence on artificial aging, a detailed understanding of these processes is of fundamental importance for tailoring the hardness of the material.

Positron annihilation spectroscopy is a very suitable technique to observe the aging behaviour of Al alloys [15]. Positrons are highly sensitive to open volume defects such as vacancies, which play an important role in the initial clustering stages. Further, transitions from coherent to semi- or incoherent precipitates can be monitored due to changes in the associated free volume. An additional benefit for the particular case of Al–Mg–Si alloys is, that positrons are captured by the precipitates, even if they do not include open volume defects. This is due to the increased positron affinity towards Mg and Si compared to Al [16–18].

In the past, positron annihilation spectroscopy has been successfully applied in studies of the microstructural changes in Al–Mg–Si alloys during age hardening [19, 20]. These include *in situ* studies in which changes in the precipitation process occured at room temperature (natural aging), and on a time scale that enabled monitoring by positron annihilation lifetime spectroscopy.

Here, we present the first *in situ* study at elevated temperatures of artificial aging (at 180 °C and 210 °C) as well as the dissolution of precipitates (>360 °C, i.e. solution heat treatment) for a commercial light weight alloy. This is achieved by *in situ* monitoring the S-parameter of the Doppler broadened positron–electron annihilation spectrum. The so-called S-parameter is used for the quantitative evaluation of the Doppler broadening spectrum of the positron–electron annihilation. It is defined as the area of the central low-momentum part of the spectrum divided by the area below the whole curve after background subtraction. The S-parameter is related to the annihilation of positrons with valence electrons of the sample. As the density of open volume defects in the sample increases, the S-parameter increases [21]. The high intensity of the positron beam at the NEPOMUC facility at FRM II enables fast spectra acquisition in order to resolve precipitation processes on very short timescales [22, 23].

The advantage of this kind of *in situ* studies compared to *ex situ* measurements is obvious. For *ex situ* studies it is necessary to measure a series of individual samples, which may vary in their composition and thus increase the uncertainty of the measurement. Further, for *ex situ* studies, each sample has to be quenched individually and kept in its particular aging state until and during the spectra acquisition. Slight variations of this procedure between different samples are unavoidable. However, by continuously *in situ* monitoring the S-parameter of only one sample during artificial aging the above mentioned uncertainties can be eliminated and the accuracy of the measurement can be increased drastically. Moreover, secondary natural aging during the spectra acquisition can be excluded, which was not the case for previous studies where the positron lifetime spectra were acquired *ex situ* at room temperature after the samples had undergone artificial aging [19]. Also the trapping behaviour might be different at low and high temperatures depending on the nature of the trapping sites. Therefore, recording positron–electron annihilation parameters at different temperatures as presented here provides more detailed insights to atomic processes.

2. Experimental

In this study a commercial-grade AW6060 Al-alloy was used in a T6 state (solution heat treatment and peak aging of the alloy) in the as-received condition. Both samples investigated were obtained from the same low-alloyed batch and were rich in magnesium (0.65at% Mg, 0.52at% Si) as revealed by optical emission spectroscopy.

In situ positron annihilation experiments were performed at the NEPOMUC high-intensity positron beamline. This positron beam provides >10^9 moderated positrons per second at an energy of 1 keV enabling a temporal resolution of the precipitation process in the alloy. All Doppler broadening spectra and corresponding S-parameter data presented here
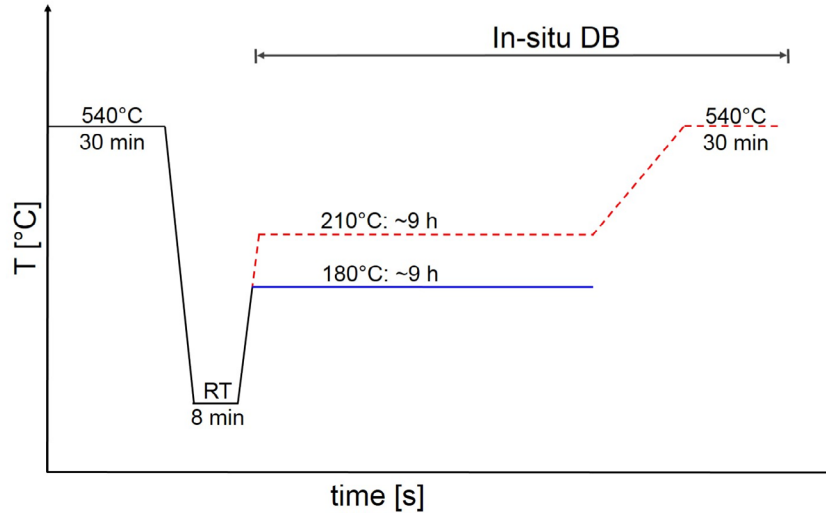
Figure 1. Sketch of the heat treatment applied to the AW6060 samples prior to and during *in situ* Doppler broadening (DB) spectroscopy.

were acquired using the Doppler broadening (DB) spectrometer [24] at the NEPOMUC beamline using four high-purity Ge detectors. The central region for calculation of the S-parameter was chosen symmetrically around the 511 keV annihilation peak from 510.15 to 511.85 keV.

The temperature program which was applied to the samples before and during the measurements is sketched in figure 1. Prior to any aging experiments, the samples were solution heat treated at $(540 \pm 1)°C$ for 30 min and subsequently water quenched to room temperature. In order to prevent natural aging, the quenched samples were stored in liquid nitrogen until mounting them into the DB spectrometer. It took approximately 8 min to reach the predefined artificial aging temperatures of 180 °C and 210 °C after removal from the liquid nitrogen bath.

In the case of artificial aging at 180 °C (210 °C) the S-parameter was first recorded for 19 min (47 min) with an integration time (time of spectra acquisition) of 15 s and a minimum of 1.3×10^5 counts per spectrum, at a fixed positron implantation energy of $E = 28$ keV. Within the following 9 hours of artificial aging (the temperature was continuously kept at 180 °C and 210 °C) for both samples the implantation energy E of the positron beam was repeatedly ramped from 0.5 keV to 28 keV within 30 min. Doppler broadening spectra were acquired with an integration time of 60 s and a minimum of 5×10^5 counts per spectrum.

Additionally for the sample aged at 210 °C, the S-parameter was recorded *in situ* during solution heat treatment directly after aging. Here the temperature was raised from 210 °C to 540 °C with a rate of approximately 8 °C min^{-1} (integration time: 60 s).

3. Results and discussion

### 3.1. Variation of the in situ Doppler broadening S-parameter during artificial aging at 180 °C and 210 °C

The *in situ* beamline measurements of the S-parameter are given in figures 2 and 3 for the artificial aging temperatures

of 180 °C and 210 °C, respectively. They are compared to the *ex situ* measurements of the mean positron lifetime τ_m, which were previously obtained from a laboratory set-up, and *in situ* dilatometric measurements of the length change $\Delta L/L$ [25].

A combined interpretation of $\Delta L/L$ and τ_m in a previous study led to the identification of three main steps in the precipitation sequence [25]. For an artificial aging temperature of 180 °C, in a first timespan A (10 s–100 s) natural aging clusters dissolve and artificial aging clusters form in the Al matrix. Next, during timespan B (100 s–11 000 s) solute clusters grow and are eventually transformed into coherent β'' precipitates. The exact time of this transformation could, however, not be verified. For proceeding artificial aging, β'' precipitates are finally transformed into semi-coherent β' precipitates (timespan C).

Also for an aging temperature of 210 °C, timespan A is attributed to the dissolution of natural aging clusters and the subsequent formation of artificial aging clusters. Contrary to the case of artificial aging at 180 °C, timespan B is skipped in this case. Due to elevated temperatures the transformation from β'' to β' precipitates sets in earlier and timespan C proceeds directly after timespan A.

In the present study, in timespan B, where no significant change of τ_m could be observed for an aging temperature of 180 °C, the S-parameter first increases significantly until it reaches an apparent maximum value at about 10^3 s. It should be noted that the next S-parameter datapoint following the maximum value at about 10^3 s is recorded 29 min later. Therefore, the position of the maximum of the S-parameter can only be estimated to be in the timespan between 10^3 s and 1.8×10^3 s. The maximum of the S-parameter is followed by a rapid decrease of the S-parameter until ca. 10^4 s which marks the end of timespan B. For aging times longer than 10^4 s the S-parameter increases again. For artificial aging at 210 °C the S-parameter shows very similar characteristics as for 180 °C. It reaches a maximum at ca. 700 s (several minutes before the end of timespan A), followed by a rapid decrease until about 2.5×10^3 s and a subsequent increase with no tendency of levelling off until 3.7×10^4 s.
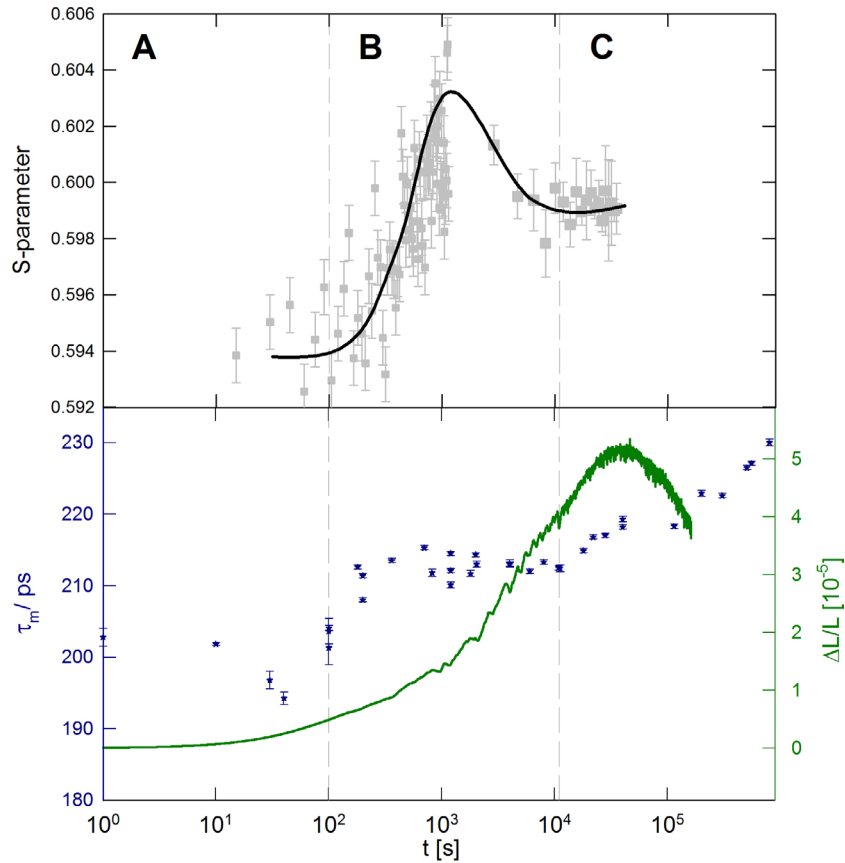
Figure 2. S-parameter (grey squares), mean positron lifetime (blue stars) and length change (solid green line) of the AW6060 sample in dependence of the artificial aging time at 180 °C. The solid black line is a guide for the eyes. The lower panel is reproduced from [25] for comparison. CC BY 4.0.

Interestingly, for both artificial aging temperatures, the variations of τ_m and the S-parameter do not coincide, which is initially unexpected, since both parameters are sensitive to the mean free volume of defects in the alloy in similar way. However, the measurement temperatures of the *ex situ* (−70 °C) and the *in situ* (180 °C/210 °C) experiments are different. Due to the high measurement temperatures during the *in situ* experiment, the variation of the S-parameter is only affected by the annihilation of positrons in deep traps, where thermal detrapping is very unlikely. On the other hand, the *ex situ* positron lifetime spectra were acquired at measurement temperatures of −70 °C, where positrons are also captured by shallow traps. Previous studies demonstrated that both trap types are present in Al-alloys during the course of aging [26]. Vacancies and larger precipitates in alloys act as deep positron traps with binding energies of about 1 eV. Shallow positron traps are clusters and small coherent precipitates which bind positrons only weakly (binding energies of about 55 meV) [26].

From previous *ex situ* positron lifetime measurements a transformation of precipitates from shallow to deep positron traps was verified. The measurements showed that after 10^3 s there are shallow traps present while after 10^4 s most of the positron traps are deep traps [27]. On the other hand, the *in situ* S-parameter includes only information about deep traps and does not give further information, neither about shallow traps nor about the ratio of shallow to deep traps. From the

initial increase of the S-parameter it can be concluded that the number of deep traps increases. At the time where the maximum S-parameter is observed this transformation of shallow to deep traps is being overshadowed by the subsequent process (the β'' transformation), but it cannot be concluded that the transformation to deep traps is finished yet.

For aging at a higher temperature (210 °C), the maximum of the S-parameter is shifted to lower aging times compared to aging at 180 °C. For both temperatures, the decrease of the S-parameter following this maximum occurs simultaneously with an increase of $\Delta L/L$. The increase of $\Delta L/L$ corresponds to an increasing number of β'' precipitates in the alloy. Thus, the maximum of the S-parameter marks the time at which the pre-β'' to β'' transformation occurs. It is likely, that remanent vacancies serving as diffusion vehicles anneal out at this point. It has to be noted that previous studies suggest that vacancies are trapped in pre-β'' precipitates, which might anneal out due to the transformation to β'' precipitates [14, 28]. In this case only a minor fraction of pre-β'' precipitates can include vacancies. If the fraction of the pre-β'' precipitates containing vacancies were pre-dominant their annealing would be visible by a decrease of τ_m, which is not the case.

Similarly, a nearly opposite behaviour of the S-parameter and τ_m was previously also observed for isochronal annealing of Al-1.9at% Cu [29]. Here, the variations of the S-parameter were caused by an agglomeration of Cu in the surroundings of the positron annihilation site. In analogy, the increase and

4
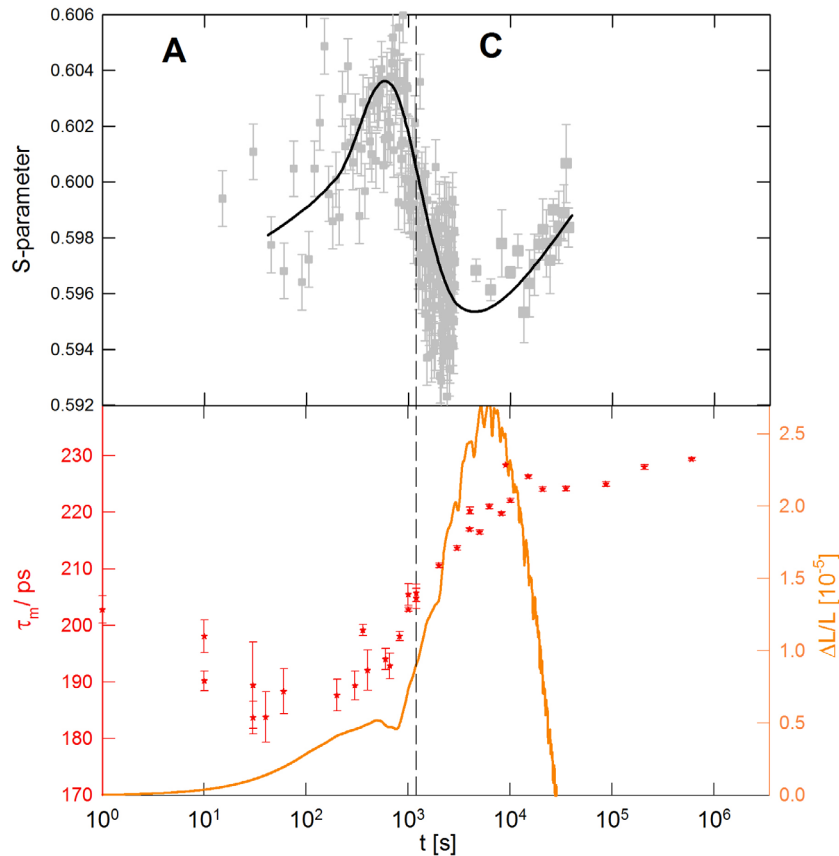
Figure 3. S-parameter (grey squares), mean positron lifetime (red stars) and length change $\Delta L/L$ (solid orange line) of the AW6060 sample in dependence of the artificial aging time at 210 °C. The lower panel is reproduced from [25] for comparison. CC BY 4.0.

subsequent decrease of the S-parameter might therefore also be interpreted as follows: For the Al–Mg–Si alloy AW6060, the formation of pre-β" precipitates, which are initially rich in Mg, can cause an increase of the S-parameter compared to Al due to a lower valence electron density [19, 30]. The subsequent decrease of the S-parameter, on the other hand, indicates an enrichment of precipitates with Si atoms upon β"-formation, which leads to an electron density increase. Indeed, indication for initially Mg-enriched pre-β" precipitates are reported for Al–Mg–Si [14]. However, in the case of AW6060, the exact composition of pre-β" precipitates is not clear yet [31, 32]. Therefore the above described, alternative interpretation is reasonable but still speculative.

The increase of the S-parameter from 2.5×10^3 s onwards at 210 °C is attributed to the transformation of β" to β' precipitates. The β' precipitates are semi-coherent and thus include a higher open volume than the coherent β" precipitates. This is also confirmed by dilatometry, where the maximum of $\Delta L/L$, corresponding to the onset of the transformation to β', occurs simultaneously to the increase of the S-parameter [33].

Again, this increase of the S-parameter can also be caused by a change of the valence electron density n_{val} as the β" precipitates transform into β' precipitates. In contrast to the situation for the pre-β"—β" transformation (see above), here it is clear that n_{val} decreases for a transformation from β"(monoclinic, $Mg_4Al_3Si_4$ [8]) to β' (hexagonal, Mg_9Si_5 [10]) precipitates. As the S-parameter varies inversely with n_{val} [30],

the observed increase of the S-parameter is consistent with a decrease of n_{val}.

For artificial aging at 180 °C and times between 10^4 s and 3×10^4 s only a slight increase of the S-parameter could be observed (see figure 2) which is, however, within the error bars of this data. Obviously, due to a slower proceeding precipitation sequence at 180 °C compared to 210 °C, the β" to β' transformation starts beyond the measuring time (which is limited to 3×10^4 s).

3.2. In situ solution heat treatment after over-aging at 210 °C

In figure 4 the temperature dependence of the S-parameter, for two nominally similar AW6060 samples, is shown during, and subsequent to, the solution heat treatment after over-aging at 210 °C. Both show a very similar behaviour of the S-parameter in dependence of the temperature demonstrating the high reproducability of the experiment. The S-parameter stays almost constant from 227 °C to 364 °C followed by a significant decrease up to 422 °C. Above 422 °C, the S-parameter increases again and shows a tendency of levelling off towards the last recorded datapoints at temperatures of 527 °C.

The decrease of the S-parameter in the temperature range from 364 °C to 422 °C can be assigned to the dissolution of the previously formed artificial aging precipitates. DSC measurements in an Al alloy, with similar Mg-to-Si ratio
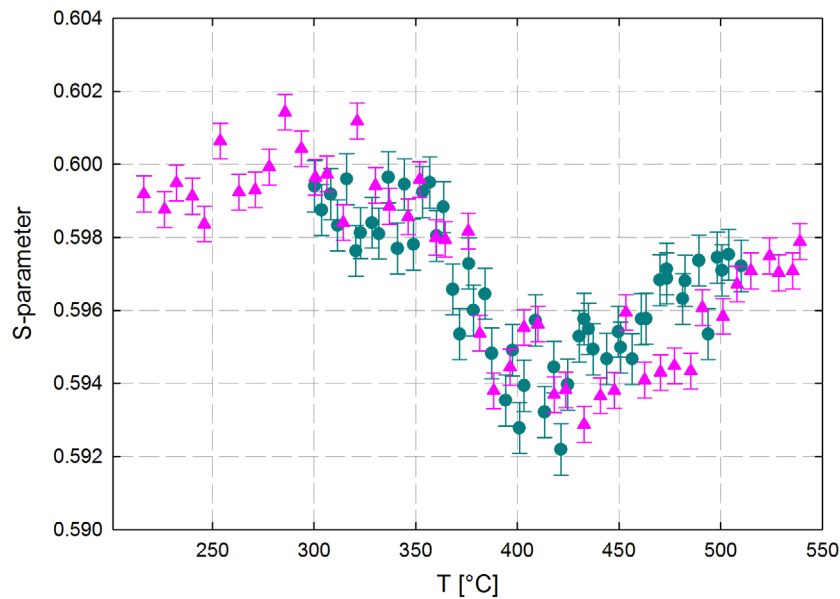
Figure 4. S-parameter of two distinct samples (sample 1: cyan dots, sample 2: pink triangles) in dependence of temperature after artificial aging at 210 °C. Note that the absolute values of sample 1 have been shifted on the vertical axis for comparison.

(AW6082) revealed the dissolution of precipitates from 397 °C to 497 °C [34].

The subsequent increase of the S-parameter above 422 °C is attributed to the generation of vacancies in the sample due to elevated temperatures. Comparing these $S(T)$ data-points to the increase of the S-parameter in dependence of the temperature for pure Al [35], in both cases similar slopes of $S(T)$ in the temperature range from 422 °C to 527 °C are observed.

4. Summary and conclusion

In this study the Doppler broadening S-parameter of an Al–Mg–Si alloy was measured *in situ* during artificial aging at 180 °C and 210 °C. In addition, the solution heat treatment after artificial aging at 210 °C was also monitored.

From an initial increase of the S-parameter until about 10^3 s (700 s) during artificial aging at 180 °C (210 °C) it can be concluded, that an increasing number of clusters, which are shallow positron traps, evolve into larger precipitates serving as deep positron traps. The subsequent decrease of the S-parameter can be attributed to a small fraction of remanent vacancies annealing out of the precipitates during the formation of β" precipitates. An alternative explanation for the initial increase and subsequent decrease of the S-parameter might be the varying Mg and Si content upon pre-β" to β"-transformation. This could, however, not be finally verified since the exact composition of pre-β" precipitates remains unclear. The recovery of the S-parameter values for times greater than 2.5×10^4 s for an artificial aging temperature of 210 °C corresponds to the transformation from β" to β' precipitates.

The S-parameter in dependence of the temperature $S(T)$, recorded during solution heat treatment, shows a decrease caused by the dissolution of precipitates from 364 °C to 422 °C. A subsequent increase of $S(T)$ from 422 °C onwards is due to thermal vacancy generation in the alloy.

ORCID iDs

L Resch ● https://orcid.org/0000-0001-5812-2869

References

[1] Miller W S, Zhuang L, Bottema J, Wittebrood A J, De Smet P, Haszler A and Vieregge A 2000 Recent development in aluminium alloys for the automotive industry *Mat. Sci. Eng.* A **280** 37–49
[2] Zhang X H, Su G, Ju G C, Wang C W and Yan W L 2010 Effect of modification treatment on the microstructure and mechanical properties of Al-0.35%Mg-7.0%Si cast alloy *Mater. Des.* **31** 4408–13
[3] Wilm A 1911 Physikalisch-metallurgische Untersuchungen über magnesiumhaltige Aluminiumlegierungen *Metall.: Z. Gesamte Hüttenkunde* **8** 225–7
[4] Duprac O H 2005 Alfred Wilm and the beginnings of Duralumin *Z. Metall.* **96** 398–404
[5] Marioara C D, Andersen S J, Zandbergen H W and Holmestad R 2005 The influence of alloy composition on precipitates of the Al–Mg–Si system *Metall. Mater. Trans.* A **36** 691–702
[6] Zandbergen M W, Xu Q, Cerezo A and Smith G D W 2015 Study of precipitation in Al–Mg–Si alloys by atom probe

tomography I. Microstructural changes as a function of ageing temperature *Acta Mater.* **101** 136–48

[7] Andersen S J, Zandbergen H W, Jansen J, Traeholt C, Tundal U and Reiso O 1998 The crystal structure of the β'' phase in Al–Mg–Si alloys *Acta Mater.* **46** 3283–98

[8] Ninive P H, Strandlie A, Gulbrandsen-Dahl S, Lefebvre W, Marioara C D, Andersen S J, Friis J, Holmestad R and Løvvik O M 2014 Detailed atomistic insight into the β'' phase in Al–Mg–Si alloys *Acta Mater.* **69** 126–34

[9] Frøseth A G, Høier R, Derlet P M, Andersen S J and Marioara C D 2003 Bonding in MgSi and Al–Mg–Si compounds relevant to Al–Mg–Si alloys *Phys. Rev.* B **67** 224106

[10] Vissers R, van Huis M A, Jansen J, Zandbergen H W, Marioara C D and Andersen S J 2007 The crystal structure of the β' phase in Al–Mg–Si alloys *Acta Mater.* **55** 3815–23

[11] Andersen S J, Marioara C D, Frøseth A, Vissers R and Zandbergen H W 2005 Crystal structure of the orthorhombic U2-Al$_4$Mg$_4$Si$_4$ precipitate in the Al–Mg–Si alloy system and its relation to the β' and β'' phases *Mat. Sci. Eng.* A **390** 127–38

[12] Andersen S J, Marioara C D, Vissers R, Frøseth A and Zandbergen H W 2007 The structural relation between precipitates in Al–Mg–Si alloys, the Al-matrix and diamond silicon, with emphasis on the trigonal phase U1-MgAl2Si2 *Mat. Sci. Eng.* A **444** 157–69

[13] Geisler A H and Hill J K 1948 Analyses and interpretations of x-ray diffraction effects in patterns of aged alloys *Acta Crystallogr.* **1** 238–52

[14] Edwards G A, Stiller K, Dunlop G L and Couper M J 1998 The precipitation sequence in Al–Mg–Si alloys *Acta Mater.* **46** 3893–904

[15] Dupasquier A, Kögel G and Somoza A 2004 Studies of light alloys by positron annihilation techniques *Acta Mater.* **52** 4707–26

[16] Staab T E M, Krause-Rehberg R, Hornauer U and Zschech E 2006 Study of artificial aging in AlMgSi (6061) and AlMgSiCu (6013) alloys by positron annihilation *J. Mater. Sci.* **41** 1059–66

[17] Dlubek G 1987 Positron studies of decomposition phenomena in Al alloys *Mater. Sci. Forum* **13** 11–32

[18] Puska M J, Lanki P and Nieminen R M 1989 Positron affinities for elemental metals *J. Phys.: Condens. Matter* **1** 6081

[19] Banhart J, Liu M, Yong Y, Liang Z, Chang C S T, Elsayed M and Lay M D 2012 Study of ageing in Al–Mg–Si alloys by positron annihilation spectroscopy *Physica* B **407** 2689–96

[20] Klobes B, Korff B, Balarisi O, Eich P, Haaks M, Maier K, Sottong R, Hühne S M, Mader W and Staab T E M 2010 Probing the defect state of individual precipitates grown in an Al–Mg–Si alloy *Phys. Rev.* B **82** 054113

[21] Krause-Rehberg R and Leipner H S 1999 *Positron Annihilation in Semiconductors* (New York: Springer)

[22] Hugenschmidt C, Löwe B, Mayer J, Piochacz C, Pikart P, Repper R, Stadlbauer M and Schreckenbach K 2008 Unprecedented intensity of a low-energy positron beam *Nucl. Instrum. Methods* A **593** 616–8

[23] Hugenschmidt C, Ceeh H, Gigl T, Lippert F, Piochacz C, Reiner M, Schreckenbach K, Vohburger S, Weber J and Zimnik S 2014 Positron beam characteristics at nepomuc upgrade *J. Phys.: Conf. Ser.* **505** 012029

[24] Gigl T, Beddrich L, Dickmann M, Rienäcker B, Thalmayr M, Vohburger S and Hugenschmidt C 2017 Defect imaging and detection of precipitates using a new scanning positron microbeam *New J. Phys.* **19** 123007

[25] Resch L, Klinser G, Hengge E, Enzinger R, Luckabauer M, Sprengel W and Würschum R 2018 Precipitation processes in Al–Mg–Si extending down to initial clustering revealed by the complementary techniques of positron lifetime spectroscopy and dilatometry *J. Mater. Sci.* **53** 14657–65

[26] Klobes B, Maier K and Staab T E M 2015 Early stage ageing effects and shallow positron traps in Al–Mg–Si alloys *Phil. Mag.* **95** 1414–24

[27] Resch L, Klinser G, Sprengel W and Würschum accepted R 2018 Identification of different positron trapping sites during artificial aging of a commercial light weight alloy *AIP Conf. Proc.* accepted

[28] Kelly A and Nicholson R B 1963 Precipitation hardening *Prog. Mater. Sci.* **10** 151

[29] Gläser U H, Dlubek G and Krause R 1991 Vacancies and precipitates in Al-1.9 at% Cu studied by positrons *Phys. Status Solidi* b **163** 337–43

[30] Dannefaer S, Puff W and Kerr D 1997 Positron line-shape parameters and lifetimes for semiconductors: systematics and temperature effects *Phys. Rev.* B **55** 2182

[31] Van Huis M A, Chen J H, Zandbergen H W and Sluiter M H F 2006 Phase stability and structural relations of nanometer-sized, matrix-embedded precipitate phases in Al–Mg–Si alloys in the late stages of evolution *Acta Mater.* **54** 2945–55

[32] Marioara C D, Andersen S J, Jansen J and Zandbergen H W 2001 Atomic model for GP-zones in a 6082 Al–Mg–Si system *Acta Mater.* **49** 321–8

[33] Hengge E, Enzinger R, Luckabauer M, Sprengel W and Würschum R 2018 Quantitative volumetric identification of precipitates in dilute alloys using high-precision isothermal dilatometry *Phil. Mag. Lett.* **98** 301–9

[34] Osten J, Milkereit B, Schick C and Kessler O 2015 Dissolution and precipitation behaviour during continuous heating of Al–Mg–Si alloys in a wide range of heating rates *Materials* **8** 2830–48

[35] Schaefer H E, Gugelmeier R, Schmolz M and Seeger A 1987 Positron lifetime spectroscopy and trapping at vacancies in aluminium *Mater. Sci. Forum* **15** 111–6 (Trans Tech Publ)